Proceedings of the 2007 IEEE
International Symposium on Assembly and Manufacturing
Ann Arbor, Michigan, USA, July 22-25, 2007

Study of cylinder/plan capillary force near millimeter scale and experimental validation

Julien Vitard, Stéphane Régnier
Laboratoire de Robotique de Paris,
28 route du Panorama – BP 61,
92265 Fontenay aux Roses, France
{vitard, regnier}@robot.jussieu.fr

Pierre Lambert
Service Beams, Université libre de Bruxelles,
CP165/14, avenue F.D. Roosevelt 50,
1050 Bruxelles
Pierre.Lambert@ulb.ac.be

***Abstract*— The theoretical study presented in this paper aims at proposing two capillary forces models related to manipulation of cylindrical and prismatic components. The underlying application framework is related to the objectives of the European NanoRAC project, which are the manipulation and characterization of nanocomponents such as nanotubes or nanowires. The analytical equivalence of Laplace and energetical method in the case of prism/plane interaction has been demonstrated, and then applied numerically to the cylinder/plane interaction. First experiments at millimeter scale on cylinders are introduced.**

I. INTRODUCTION

A lot of work has been reported on capillary forces modelling based on energetic method or a direct force computation from the meniscus geometry obtained by numerically solving the so-called Laplace equation or approximated by a geometrical profile (circle, parabola). More information can be found in [1]. This paper aims at proving that the capillary force obtained by derivingthe interfacial energy is exactly equal to the sum of Laplace and tension terms, clarifying models presented in [2], [3], [4]. This is proven by qualitative arguments, section II presents analogy and difference between both study cases : prism and cylinder, an analytical proof is given, in section III, for the case of the interaction between a prism and a plane, section IV presents Laplace method applied to the cylinder, and some numerical results. Section V presents first results at millimeter scale.

II. CYLINDER/PRISM ANALOGY AND DIFFERENCE

This section aims at defining the meniscus shape equation, and calculating the volume of liquid, for both geometries interactions : prism and cylinder interacting with a plane.

A. Meniscus shape

Let us describe some notations used in Fig. 1, θ_1 and θ_2 are the contact angles between liquid and, respectively, the plane and the prism (or the cylinder), z is the distance between the object and the plane, ϕ represents the aperture angle for the prism and the immersion angle for the cylinder (fig. 2), h is the immersion height, α is the sum of both angles ϕ and θ_2, x_1 and x_2 are positions of the contact line with liquid.

Both interaction models presented here below are based on a simplification of the Laplace equation giving the pressure difference across the liquid-vapor interface $p_{in} - p_{out}$ as a function of the surface tension γ and the meniscus curvature H [5] :

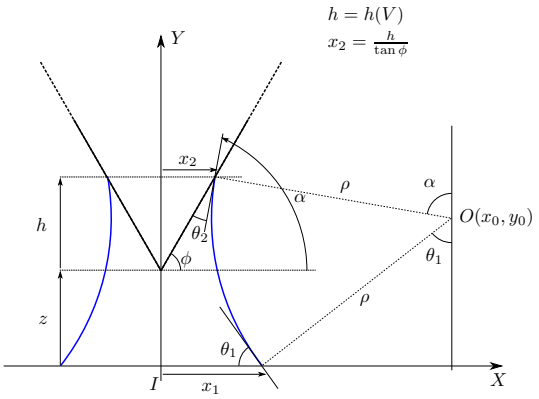

Fig. 1. 2D notations for Prism/Plan interactions

$$2\gamma H = p_{in} - p_{out} \tag{1}$$

which can be rewritten into :

$$\gamma\left(\frac{1}{R_1} + \frac{1}{R_2}\right) = p_{in} - p_{out} \tag{2}$$

where $(\frac{1}{R_1} + \frac{1}{R_2})$ represent the double of the mean curvature H.

Since the prism and the cylinder are defined along the Z axis perpendicular to I_{XY}, the curvature of the meniscus in this direction is null and the Laplace equation becomes :

$$\frac{x''}{(1 + x'^2)^{\frac{3}{2}}} = \frac{\Delta p}{\gamma} \tag{3}$$

whose left hand side represents the meniscus curvature in the O_{XY} plane ($[\ ]' = \frac{d[\ ]}{dy}$). The second term is assumed to be constant (*i.e.* the so-called Bond number $\ll 1$) and this equation can be integrated twice with respect to y, to find the expression of the meniscus profile in the O_{XY} plane.

An easier way to understand the shape of the meniscus is based on the fact that a curve with a constant curvature is a circle, whose radius will be noted ρ, center coordinates are (x_0, y_0), and equation is given by :

$$x = x_0 - \sqrt{\rho^2 - (y_0 - y)^2} \tag{4}$$

It can be deduced from Fig. 1 that :

$$\rho = \frac{z+h}{\cos\theta_1 + \cos\alpha} \quad (5)$$

$$y_0 = \rho\cos\theta_1 \quad (6)$$

$$x_0 = x_2 + (-y_0 + z + h)\tan\alpha \quad (7)$$

Note that in equations 5-7, h, θ_1, α are given.

$$x_2 = \frac{h}{\tan\phi}$$

where ϕ is given and h is to be determined from the known volume of liquid V (see further equation 15) To summarise, using the circle description, eq.: 3 can be simplified as :

$$\frac{1}{\rho} = \frac{\Delta p}{\gamma} \quad (8)$$

Note that this simplified expression is exact in the prismatic chosen case and can be used as an approximation for sphere/plane interaction when the curvature radius ρ is much smaller than the neck radius $\rho' = \min(x)$, which is the case for small gap z.

B. Liquid volume

As already stated, the liquid volume V will be used to find (i) the immersion height h in the case of the prism and (ii) the immersion angle ϕ in the case of cylinder. In both cases, V is written as :

$$V = 2L\int_0^{z+h} x(y)\,dy - v^i \quad (9)$$

where $x(y)$ is given by eq. 4, L is the object's length and v^i is the prism volume v^{pr} or cylinder volume v^{cyl} to remove ([1]) :

$$v^{pr} = Lx_2h \quad (10)$$

$$v^{cyl} = LR^2(\phi - \mathrm{cs}\ \phi) \quad (11)$$

Equation 9 can be rewritten as eq. 12 and implies evaluation of the integral noted I in eq. 13 :

$$\begin{aligned} V &= 2L\int_0^{z+h}\left[x_0 - \sqrt{\rho^2 - (y_0 - y)^2}\right]dy - v^i \\ &= 2Lx_0(z+h) - v^i - 2L\int_0^{z+h}\sqrt{\rho^2 - (y - y_0)^2}\,dy \end{aligned} \quad (12)$$

using the substitution $u \equiv y - y_0$,

$$\begin{aligned} I &= \int_{-y_0}^{-y_0+z+h}\sqrt{\rho^2 - u^2}\,du \\ &= \left[\frac{\rho^2}{2}\mathrm{asin}\frac{u}{\rho} + \frac{u}{2}\sqrt{\rho^2 - u^2}\right]_{-y_0}^{-y_0+z+h} \end{aligned} \quad (13)$$

Using equations 5-6, eq. 13 can be rewritten as :

$$I = \frac{\rho^2}{2}(\pi - \alpha - \theta_1 + \mathrm{cs}\ \alpha + \mathrm{cs}\ \theta_1) \quad (14)$$

[1] cs $x \equiv \cos(x)\sin(x)$ is used as notation in the whole document

and, consequently,

$$\begin{aligned} V &= 2Lx_0(z+h) - v^i \\ &\quad -L\rho^2(\pi - \alpha - \theta_1 + \mathrm{cs}\ \alpha + \mathrm{cs}\ \theta_1) \end{aligned} \quad (15)$$

Using expression of x_0 in eq. 7 and the appropriate volume v^i , the expression of liquid volume (10-11) can now be deduced from equation 15.

III. STUDY CASE: PRISM/PLAN INTERACTION

This section aims at applying the Laplace based and energetic force model, using the geometrical results of section II.

A. Laplace approach

Using eq. 15 and prism parameters, the expression of volume V becomes:

$$V = 2Lz\frac{h}{\tan\phi} + L\frac{h^2}{\tan\phi} + L(z+h)^2\mu \quad (16)$$

$$\text{with} \quad \mu = \frac{\mathrm{cs}\ \alpha + 2\sin\alpha\cos\theta_1 - \pi + \alpha + \theta_1 - \mathrm{cs}\ \theta_1}{(\cos\theta_1 + \cos\alpha)^2}$$

The previous equation can be rewritten into a second degree equation in h whose positive solution gives the immersion height :

$$h^2 + 2hz + \frac{z^2\mu - \frac{V}{L}}{\frac{1}{\tan\phi} + \mu} = 0 \quad (17)$$

$$h = -z + \sqrt{z^2 - \frac{z^2\mu - \frac{V}{L}}{\frac{1}{\tan\phi} + \mu}} \quad (18)$$

The capillary force can be written as the sum of a term depending on the Laplace pressure difference Δp and the so-called tension term :

$$\begin{aligned} F &= 2x_1L\Delta p + 2L\gamma\sin\theta_1 \\ &= 2\left(x_0 - y_0\tan\theta_1\right)L\frac{\gamma}{\rho} + 2L\gamma\sin\theta_1 \\ &= 2\left(\frac{h}{\tan\phi} + \rho\sin\alpha - \rho\sin\theta_1\right)L\frac{\gamma}{\rho} + 2L\gamma\sin\theta_1 \\ &= 2L\gamma\left(\frac{h}{\rho\tan\phi} + \sin\alpha - \sin\theta_1\right) + 2L\gamma\sin\theta_1 \\ &= 2L\gamma\left(\frac{h}{\rho\tan\phi} + \sin\alpha\right) \end{aligned} \quad (19)$$

$$F = 2L\gamma\left(\frac{h}{h+z}\left(\frac{\cos\theta_1 + \cos\alpha}{\tan\phi}\right) + \sin\alpha\right) \quad (20)$$

B. Energetical approach

The energetical method is based on the derivation of the total interfacial energy W given by :

$$W = \gamma\Sigma + \sum_{pr,pl} A^i_{SV}\gamma^i_{SV} + \sum_{pr,pl} A^i_{SL}\gamma^i_{SL} + C \quad (21)$$

where γ is the surface tension, Σ is the liquid-vapor area, A^i_{SV} (A^i_{SL}) is the solid-vapor (solid-liquid) area on solid i, γ^i_{SV} (γ^i_{SL}) is the solid-vapor (solid-liquid) interfacial energy and C is an arbitrary constant, which will be discarded by derivation at the next step.

For the prism/plane interaction, the different surfaces are given by :

$$\Sigma = 2\rho(\pi-\alpha-\theta_1)L \quad (22)$$
$$A_{SL}^{pr} = 2L\frac{h}{\sin\phi} \quad (23)$$
$$A_{SL}^{pl} = 2x_1L \quad (24)$$
$$A_{SV}^{pr} = 2L\frac{K-h}{\sin\phi} \quad (25)$$
$$A_{SV}^{pl} = 2(r-x_1)L \quad (26)$$

K and r in equations 25-26 represent arbitrary distance to calculate interaction surfaces.

Using the Young-Dupré equation, interfacial energies can be replaced by contact angles (see Fig.1) and surface tension :

$$\gamma_{SV}^{i} - \gamma_{SL}^{i} = \gamma\cos\theta_i \quad (27)$$

The expression of the total interfacial energy (eq. 21) can be rewritten as follows :

$$W = 2L\left(\frac{h}{\sin\phi}(\gamma_{SL}^{pr}-\gamma_{SV}^{pr}) + x_1(\gamma_{SL}^{pl}-\gamma_{SV}^{pl}) + \rho(\pi-\alpha-\theta_1)\gamma\right) + \underbrace{\left[2L\frac{H}{\sin\phi}\gamma_{SV}^{pr} + 2rL\gamma_{SV}^{pl}\right]}_{C} \quad (28)$$

This equation can be rewritten, using eq. 27, into :

$$W = 2L\gamma\left(-\frac{h}{\sin\phi}\cos\theta_2 - x_1\cos\theta_1 + \rho(\pi-\alpha-\theta_1)\right) + C \quad (29)$$

$$\text{using} \quad x_1 = x_0 - y_0\tan\theta_1 \quad (30)$$

$$W = \left(\frac{z+h}{\cos\theta_1+\cos\alpha}(\pi-\alpha-\theta_1-\sin\alpha\cos\theta_1+\text{cs }\theta_1) - h\left(\frac{\cos\theta_1}{\tan\phi}+\frac{\cos\theta_2}{\sin\phi}\right)\right)2L\gamma \quad (31)$$

$$W = 2L\gamma\left((z+h)\beta - h\left(\frac{\cos\theta_1}{\tan\phi}+\frac{\cos\theta_2}{\sin\phi}\right)\right) \quad (32)$$

$$\text{with} \quad \beta = \frac{\pi-\alpha-\theta_1-\sin\alpha\cos\theta_1+\text{cs }\theta_1}{\cos\theta_1+\cos\alpha}$$

To obtain the capillary force, expression 32 will be derived according to z, since the term noted C is constant, it can be left. Variation of h with respect to z can be deduced assuming $\frac{dV}{dz} = 0$ from eq. 18 :

$$\frac{dh}{dz} = -1 + \frac{z}{z+h}\frac{1}{1+\mu\tan\phi} \quad (33)$$

The expression of derivate of W according to z using derivate of h (see eq. 33) :

$$\frac{dW}{dz} = 2L\gamma\left[\frac{\cos\theta_1}{\tan\phi}+\frac{\cos\theta_2}{\sin\phi} + \frac{z}{z+h}\left(\beta-\frac{\cos\theta_1}{\tan\phi}-\frac{\cos\theta_2}{\sin\phi}\right)\frac{1}{1+\mu\tan\phi}\right] \quad (34)$$

And finally, the expression of capillary force F is given by :

$$F = -\frac{dW}{dz} \quad (35)$$

C. Equivalence of both methods

In order to show equivalence between both methods, equations 20 and 35 need to be equal. In equation 34 (energetical method), the term factor of $\frac{z}{z+h}$ can be expressed as:

$$\left(\beta-\frac{\cos\theta_1}{\tan\phi}-\frac{\cos\theta_2}{\sin\phi}\right)\frac{1}{1+\mu\tan\phi} = -\frac{\cos\theta_1+\cos\alpha}{\tan\phi} \quad (36)$$

Equation 34 can be rewritten into

$$\frac{1}{2L\gamma}\frac{dW}{dz} = \frac{\cos\theta_1}{\tan\phi}+\frac{\cos\theta_2}{\sin\phi} - \frac{z}{z+h}\frac{\cos\theta_1+\cos\alpha}{\tan\phi} \quad (37)$$

By substracting and adding $\sin\alpha$ to the latter equation, the expression of force can be found :

$$\frac{1}{2L\gamma}\frac{dW}{dz} = \frac{h}{h+z}\left(\frac{\cos\theta_1+\cos\alpha}{\tan\phi}\right)+\sin\alpha$$

For the prism/plan interaction, both methods are identical, it can also be shown numerically for the interaction between cylinder and plan.

IV. REAL CASE: CYLINDER/PLAN INTERACTION

A. Laplace approach

Using expression 15 and cylinder parameters (see Fig. 2), a mathematical relation similar to 16 can be found between V and h.

Unfortunately, h cannot be found analytically[2] and a numerical algorithm is needed to perform ϕ calculus.

The capillary force expression is deduced from relation 19 and is given by :

$$F = 2L\gamma\left(R\frac{\cos\theta_1+\cos\alpha}{z+R(1-\cos\phi)}\sin\phi+\sin\alpha\right) \quad (38)$$

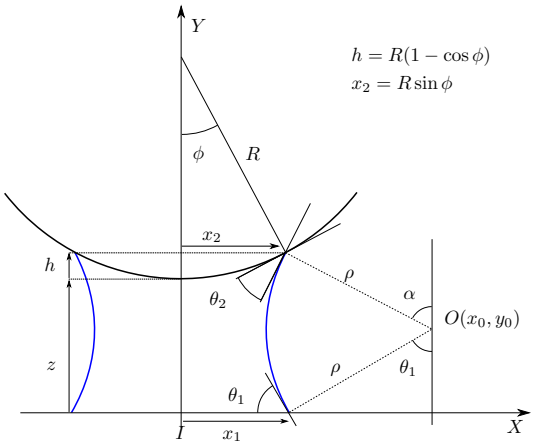

Fig. 2. 2D notations for Cylinder/Plan interactions

[2]that is the reason why this relation has been studied, because it has an analytical solution in the case of prism/plane interaction.

B. Numerical Equivalence

By applying the energetical method, an expression of W similar to eq. 32 is found. But now, the filling angle ϕ depends on volume V and separation distance z, and need to be extracted numerically.

The algorithm shown in Fig. 3 computes, for a given set of parameters, the angle ϕ, and the energy W. The capillary force can then be deduced using the derivative expression of energy W.

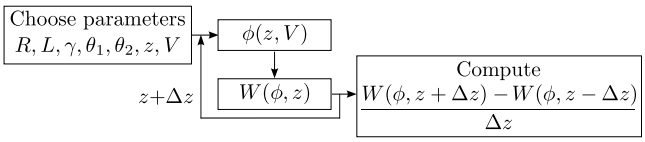

Fig. 3. Derivative algorithm

Both approaches, energetical and Laplace, are compared on Fig. 4 by plotting normalised capillary force $\overline{F} = F/2L\gamma$ against ratio z/L.

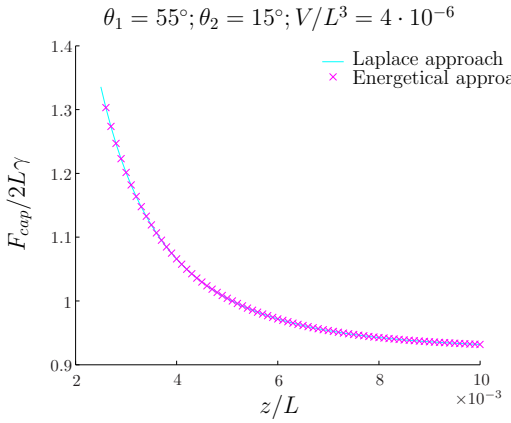

Fig. 4. Numerical equivalence between both approach

The conclusion of it is howewer to proove the equivalence of both force model once again. Since the Laplace approach is easier, expression 38 will be used in what follows.

C. Numerical Results

In figure 5, the normalised capillary force $\overline{F} = F/2L\gamma$ is expressed using adimensionnal numbers : θ_1, θ_2, V/L^3, z/L and R/L, then it is plotted versus the ratio z/L.

Fig. 5(a) shows variations of force $\overline{F}$ with the ratio V/L^3. The capillary force $\overline{F}$ seems to increase when the volume V and the separation distance z decrease. For higher values of ratio z/L and ratio V/L^3, the force $\overline{F}$ converges towards 1.

Fig. 5(b) shows variations of force $\overline{F}$ with the contact angles θ_1=θ_2($\equiv \theta_s$). For a ratio z/L larger than 1 the force $\overline{F}$ seems to remain constant for all values of θ_s, towards $\overline{F} \approx 1$. For small values of θ_s, the force increases slowly when z/L decreases. When values of θ_s increase and the ratio z/L decreases, the force $\overline{F}$ decreases rapidly until the ratio $z/L = 1$, and slowly after this ratio.

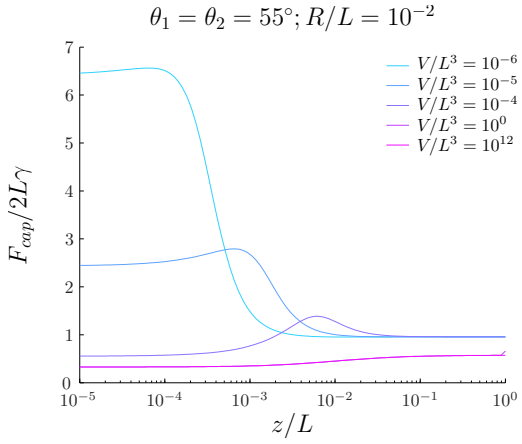

(a) $\overline{F} = f(z/L, V/L^3)$

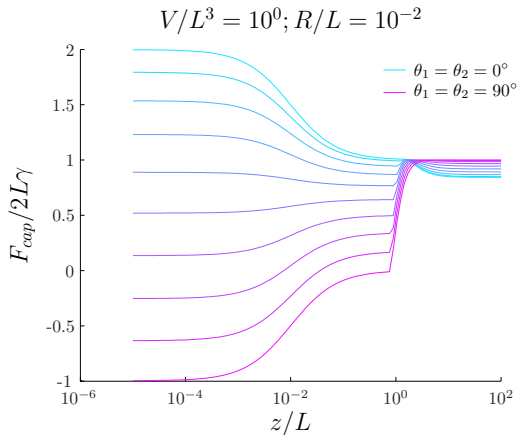

(b) $\overline{F} = f(z/L, \theta_1 = \theta_2)$

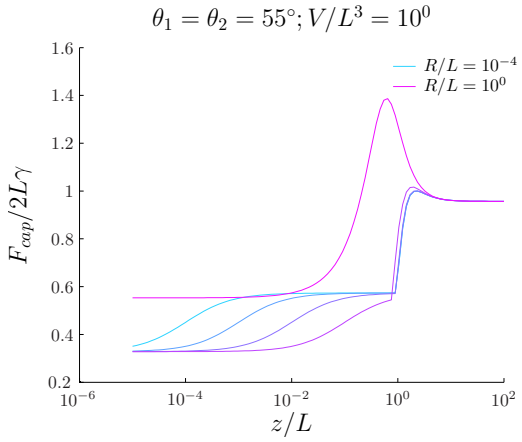

(c) $\overline{F} = f(z/L, R/L)$

Fig. 5. Abacus for Cylinder/Plan interaction

Fig. 5(c) shows variations of force $\overline{F}$ with the ratio R/L. There is also a different behaviour near the ratio z/L=1, towards z/L=1 (superior values), the capillary force increases to pass through a maximum, after this peak, the force decreases to remain constant when the separation distance z decreases. The value of the peak increases when the ratio R/L decreases.

V. EXPERIMENTAL VALIDATION

This section aims at presenting firsts results obtained with different cylinder-component-liquid combinations at the millimeter-scale.

A. Short description of experimental set up

The test bench simply consists on measuring the force between a gripper and a calibrated blade, on which a small droplet of liquid is deposited. Vertical displacement of the gripper and deflection of the blade are measured using non contact diplacement sensors. The system presented on Fig. 6 is fully described in [6].

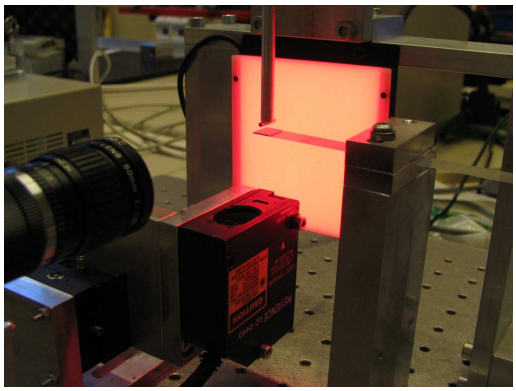

Fig. 6. Experimental force measurement set up.

B. Experiments as entries of model

1) Static contact angles: As the contact angles θ_i constitute inputs for the models, it was necessary to measure them according to the different solid-liquid combinations.

For each configuration, the meniscus have been imaged 5 times for advancing and receding contact angle and angles were measured 3 or 4 times. This was achieved with an almost zero (a few μms^{-1}) velocity.

TABLE I

ADVANCING AND RECEDING CONTACT ANGLES.

Liquid	Solid	θ_A (°)	θ_R (°)	σ_{θ_A} (°)	σ_{θ_R} (°)
H_2O (I)	St	93.6	62.1	7.1	3
H_2O (I)	Si	55.4	28.2	12.5	3
H_2O (I)	GC-St-0x	86.7	55	3.8	10
Oil (II)	St	26	16.7	3.2	2.9
Oil (II)	Si	29	17.8	7.6	3.7
Oil (II)	GC-St-0x	21.8	17.3	4.8	3.4

The results are presented in Table I where liquid I was water ($\gamma = 72 mNm^{-1}$) and liquid II was silicon oil (R47V50, $\gamma = 20.8 mNm^{-1}$). The two tested components were steel (St) and silicon (Si) blades. Grippers were steel cylinders (GC-St-0x) of 2 and 3 mm of diameter with a length of 11.9 mm. The measured angles have been averaged (θ_A and θ_R) and their standard deviations computed (σ_{θ_A} and σ_{θ_R}).

2) Volume of liquid: The liquid amount is calibrated with a manual dispensing device (from 0.1 to 2.5µL with steps equal to 2nL) or it can be estimated by surimposing the simulated meniscus on the experimental meniscus shape (see Fig. 7(a)). The volume V, depending on ϕ and z, can be calculated with an expression similar to 16 as briefly described in section IV-B.

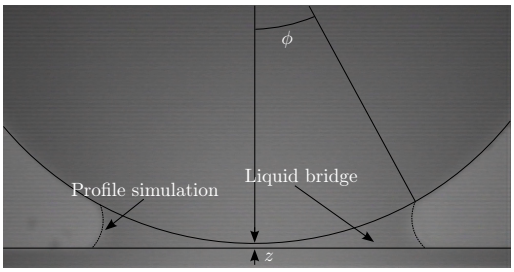

(a) Volume measurement from meniscus picture

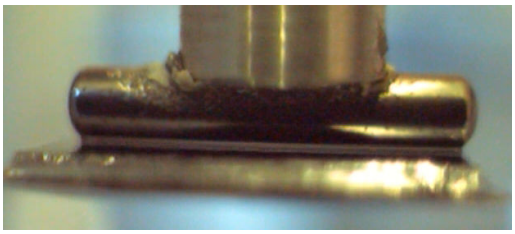

(b) Meniscus along cylinder axis

Fig. 7. Meniscus view, front (a) and side (b)

Fig. 7(b) presents a side view of a 0.5µL silicon oil meniscus obtained between a steel cylinder and a Si blade. For this configuration, the meniscus profile is along the cylinder axis as expected in the model.

C. Force at contact

This section briefly presents the force at contact curve, obtained when the gap between the cylinder and the component is equal to zero ($z = 0$). Fig.8 shows the force F versus the volume V, the model is in good agreement for small diameter and large volume of liquid.

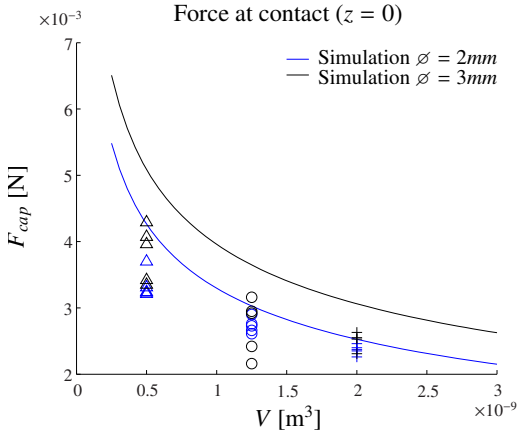

Fig. 8. Force at contact for GC-Si-0x with silicon oil, experimental points for $V = 0.5\mu L$ (△), $V = 1.25\mu L$ (○), $V = 2\mu L$ (+)

D. Force-distance curve

This section presents simulations and experimental results of force-distance curves realised with a gap z different from zero. Fig. 9 shows the capillary force F plotted versus the gap z, the force is exerted by a 2mm ⌀ cylinder on a silicon component for different volume of silicon oil.

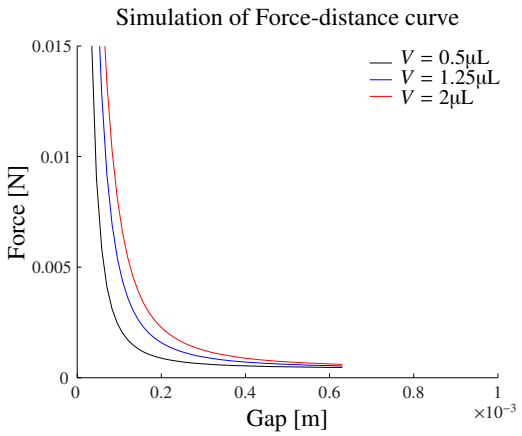

Fig. 9. Force-distance curve GC-Si-02 configuration with silicon oil.

Increasing the separation distance between the cylinder and the component will decrease the force, it means that the sticking effect due to capilary force can be reduced or suppressed by increasing the gap.

Fig. 10 shows experimental force-distance curves realised with a 15mm ⌀ Aluminium cylinder on a Si blade for different volumes of silicon oil: 10µL (△), 20µL (○), and 30µL (+).

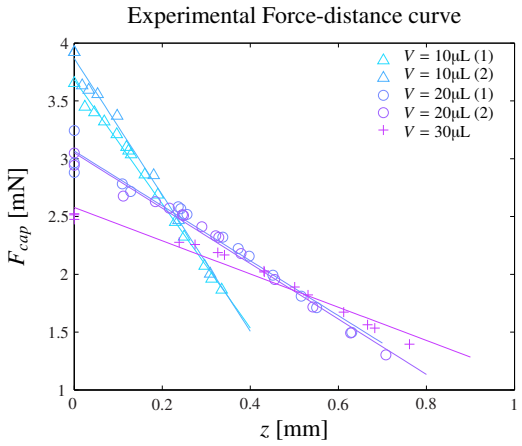

Fig. 10. Force-distance curve

Two sets of datas are presented for volumes 10 and 20µL, denoting a good reproducibility of the capillary force measurement.

We can notice that the force at contact for $z = 0$ decreases when the volume of liquid increases. The capillary force increases when the volume V and the separation distance z decrease.

VI. CONCLUSION

As a conclusion, it has been demonstrated analytically that using the simple prism/plan interaction, Laplace approach and energetical approach are equivalent in order to evaluate the capillary force. This result has been used to show numerically the same equivalence in the case of the cylinder/plan interaction.

First experiments at the millimeter-scale show a good approximation by the model, of the force at contact, for small diameter and large volume. Simulations of force-distance curve presented in this paper need to be verified in future experiments.

Further experiments need to be undertaken in order to proove or refute the application of this model at a lower scale, to describe, for example, nanowires/plane interactions with a liquid layer.

References

[1] P. Lambert and A. Delchambre, "Parameters Ruling Capillary Forces at the Submillimetric Scale," *Langmuir*, vol. 21, no. 21, pp. 9537–9543, 2005.

[2] A. Marmur, "Tip-surface capillary interactions," *Langmuir*, vol. 9, no. 7, pp. 1922–1926, 1993.

[3] A. de Lazzer, M. Dreyer, and H. J. Rath, "Particle-Surface Capillary Forces," *Langmuir*, vol. 15, no. 13, pp. 4551–4559, 1999.

[4] Y. I. Rabinovich, M. S. Esayanur, and B. M. Moudgil, "Capillary Forces between Two Spheres with a Fixed Volume Liquid Bridge: Theory and Experiment," *Langmuir*, vol. 21, no. 24, pp. 10 992–10 997, 2005.

[5] A. W. Adamson and A. P. Gast, *Physical Chemistry of Surfaces*, 6th ed., J. Wiley and Sons, Eds., 1997.

[6] P. Lambert, "A Contribution to Microassembly: A Study of Capillary Forces as a Gripping Principle," Ph.D. dissertation, Université libre de Bruxelles, Bruxelles, Belgium, 2004.